Published in final edited form as:
Genesis. 2012 December ; 50(12): 871–881. doi:10.1002/dvg.22051.

Craniofacial abnormalities result from knock down of nonsyndromic clefting gene, *crispld2*, in zebrafish

Qiuping Yuan[1], **Brett T. Chiquet**[1,2], **Laura DeVault**[1], **Matthew L. Warman**[3], **Yukio Nakamura**[4], **Eric C. Swindell**[1], and **Jacqueline T. Hecht**[1]

[1]Department of Pediatrics, University of Texas Medical School at Houston, Houston, TX

[2]Graduate School of Biological Sciences, University of Texas Health Sciences Center, Houston, Houston, TX

[3]Howard Hughes Medical Institute, Department of Genetics, Boston Children's Hospital, Boston, MA

[4]Department of Orthopaedic Surgery, Showa Inan General Hospital, Komagane, Japan

Abstract

Nonsyndromic cleft lip and palate (NSCLP), a common birth defect, affects 4000 newborns in the US each year. Previously, we described an association between *CRISPLD2* and NSCLP and showed *Crispld2* expression in the murine palate. These results suggested that a perturbation in CRISPLD2 activity affects craniofacial development. Here, we describe *crispld2* expression and the phenotypic consequence of its loss of function in zebrafish. *crispld2* was expressed at all stages of zebrafish morphogenesis examined and localized to the rostral end by 1-day post fertilization. Morpholino knockdown of *crispld2* resulted in significant jaw and palatal abnormalities in a dose dependent manner. Loss of *crispld2* caused aberrant patterning of neural crest cells (NCC) suggesting that *crispld2* is necessary for normal NCC formation. Altogether, we show that *crispld2* plays a significant role in the development of the zebrafish craniofacies and alteration of normal protein levels disturbs palate and jaw formation. These data provide support for a role of CRISPLD2 in NSCLP.

Keywords

cleft lip and palate; CRISPLD2; zebrafish; neural crest cells; craniofacial development

Introduction

Craniofacial development is a highly regulated process involving genes and environmental factors that regulate cell growth, apoptosis, nutrient supply, and the convergence and fusion of the facial and palatal processes. Disruption of any part of this process in humans may contribute to birth defects, such as nonsyndromic cleft lip with or without cleft palate (NSCLP). NSCLP is a common birth defect affecting 135,000 newborns worldwide each year (Gorlin, 2001; Wyszynski, 2002). Treatment of NSCLP requires surgical, dental and speech therapies, creating a significant healthcare burden for affected families. Therefore, identifying the etiologic causes of NSCLP and understanding how these factors contribute to the clefting phenotype is a high priority.

Corresponding Author: Jacqueline T. Hecht, PhD, University of Texas Medical School at Houston, Department of Pediatrics, PO Box 20708, Houston, TX 77030, 713-500-5764 (voice), 713-500-5689 (fax), Jacqueline.T.Hecht@uth.tmc.edu.

Previously, a small number of genes have been associated with NSCLP. These genes, including interferon regulatory factor 6 (IRF6), contribute to approximately 20% of NSCLP heritability (Blanton *et al.*, 2005; Jugessur *et al.*, 2008; Park *et al.*, 2007; Scapoli *et al.*, 2005; Srichomthong *et al.*, 2005; Vieira *et al.*, 2007; Zucchero *et al.*, 2004). We have shown and others have confirmed that the *CRISPLD2* gene is associated with NSCLP (Chiquet *et al.*, 2007; Letra *et al.*, 2010; Shen *et al.*, 2011). Additionally, we have demonstrated that *Crispld2* is expressed in the developing orofacial region of mouse embryos (Chiquet *et al.*, 2007). Crispld2, also identified as Lgl1 (late gestation lung 1), is expressed in mouse lung tissue (Kaplan *et al.*, 1999). Crispld2/Lgl1 null mice are embryonic lethal at E9.5 precluding analysis of craniofacial structures. Crispld2/Lgl1 heterozygous mice are grossly normal and no craniofacial defects were reported (Lan *et al.*, 2009). However, close inspection of the lungs from Crispld2/Lgl1 heterozygous mice exhibited delayed maturation (Lan *et al.*, 2009). Oyewumi et al. (2003) suggest that CRISPLD2 plays an important role in epithelial - mesenchymal interactions in lung tissue through its potential role as a secreted glycoprotein (Oyewumi *et al.*, 2003). Epithelial-mesenchymal interactions have previously been shown to play an important role in the transition of neuroepithelial cells to neural crest cells (NCCs) prior to migration and formation of the craniofacies, suggesting a potential role for CRISPLD2 in craniofacial development (Berndt *et al.*, 2008; Kang and Svoboda, 2005). In this study, we utilized zebrafish to define the timing and expression of *crispld2* during development and to investigate Crispld2 function.

Results

Amino acid alignment of CRISPLD2 in seven vertebrate species identified homology between all species (Fig. 1). The zebrafish Crispld2 is 60% identical to human CRISPLD2 at the amino acid level. The zebrafish Crispld2 protein is 513 amino acids in length compared to 458-504 of other species. Crispld2 contains a highly conserved secreted cysteine protein domain (SCP) as well as two highly conserved LCCL domains (Fig. 1 and 3B). Based on genomic sequence analysis, both human and zebrafish contain a single CRISPLD2 gene.

As shown in Fig. 2A, *crispld2* expression was detected early in development at 3, 4, 27 and 72 hours post fertilization (hpf). Whole mount *in situ* hybridization was performed to define expression at: 5-7 somite stage, 13-15 somite stage, 1dpf, 2dpf, 3dpf, 4dpf and 5dpf using two antisense probes. As shown in Fig. 2, *crispld2* is ubiquitously expressed during early development and localizes to the anterior part of the embryo including the craniofacial region between 1 to 5dpf. These results were confirmed using multiple riboprobes. Sections of whole mount *in situ* hybridizations confirmed ubiquitous expression in craniofacial regions of the embryo (data not shown). Embryos hybridized to a sense control riboprobe showed no staining (data not shown).

To define the significance of the loss of Crispld2 function in zebrafish, we tested four *crispld2* morpholinos (MO); one directed against the exon 3/intron 3 splice site (MO1), a second directed against the exon 4/intron 4 splice site (MO2), a third directed against the translation start site (MO3, Fig. 3A) and a mismatch control MO for MO3. Abnormal splicing in MO1 and MO2 injected embryos was confirmed by PCR amplification using primers surrounding exons 3 and 4 mRNA products (data not shown). After sequencing, these PCR products were found to contain the expected intronic sequences. Inclusion of these intronic sequences results in premature stop codons that are predicted to generate truncated protein products shown in Fig. 3B.

MO knockdown embryos had lower survival rates, at 1 and 5 dpf, when compared to uninjected control embryos. A high percentage of abnormal phenotypes were also found in these embryos when compared to uninjected control embryos. At 1 dpf, phenotypes included

failure to develop (Fig. 3D), delayed development (Fig. 3E-F) and grossly normal embryos (Fig. 3C). At 5 dpf, of those embryos that survived, a range of phenotypes was observed including severely truncated body (Fig. 3H), shortened and curved tail with cardiac edema (Fig. 3I) and grossly normal when compared to uninjected control embryos (Fig. 3G).

Alcian blue staining was used to visualize the cartilage structures of the craniofacies in all MO and uninjected control embryos at 5 and 7 dpf. Numerous anomalies were found in the injected embryos, with the most severe seen in MO3 injected embryos. For MO1 and MO2, these include a widening of ceratobranchial cartilages forming the lower jaw and malformations in the Meckel and palatoquadrate cartilages (Fig. 4B, C, J and K) compared to uninjected embryos (Fig. 4A and I) and control MO injected embryos (data not shown) both of which showed no phenotypes. MO3 injected embryos show a complete loss of lower jaw structures (Fig. 4D, L). In addition, we observed a wide variety of malformations of the palate in MO injected embryos (Fig 4F-H, N-P), but not in uninjected embryos (Fig 4E and M) and MO control injected embryos (data not shown). Injection of MO1 and MO2 produced mild abnormalities of the palate, including anterior and posterior clefting of the ethmoid plate (ep) as well as reduction of the hypophyseal fenestra (hf) (red arrows in Fig. 4F, G, N and O). Injection of MO3 produced more severe abnormalities including the complete loss of the ethmoid plate and hypophyseal fenestra as well as severe reduction of the trabeculae (tc) (arrow in Fig. 4 H, P). MO3 knockdown resulted severe phenotypes in 72% of injected embryos compared to MO1 and MO2 that had 2% and 38% severe phenotypes, respectively (Table 1). Increasing the amount of MO3 injected resulted in more severe cartilage defects (Fig 5B-D and F-H) while injection of the control MO at similar concentrations showed no effect, similar to uninjected controls (Fig 5A, 5E and data not shown). In addition, co-injection of MO3 with a p53 morpholino resulted in similar severe palatal and jaw phenotypes, confirming that this phenotype is not an artifact of morpholino induced cell death. (Supplemental Fig. 1) (Robu *et al.*, 2007). The severe phenotype seen upon injection of MO3 is fully rescued by co-injection of a full-length zebrafish *crispld2* mRNA, further proving the specificity of MO3 for zebrafish *crispld2* (Supplemental Fig. 2). To determine the effect of MO3 injection on Crispld2 protein levels, we show a decrease of Crispld2 protein levels in MO3 injected embryos as compared to uninjected controls (UIC) while levels of a loading control, Gapdh, remain unchanged (Supplemental Fig. 3). The severity of the phenotype seen with MO3 is likely due to the fact that MO3 should result in the knockdown of both maternal and zygotic protein while MO1 and MO2 should only affect the processing of zygotic mRNA resulting in the truncated mRNAs described in Fig. 3B. Maternal mRNA should not be affected in MO1 and MO2 injected embryos. In addition, the truncated proteins translated from truncated mRNAs in MO1 and MO2 injected embryos might retain some residual activity. Analysis of the different *crispld2* protein products as well as extent of Crispld2 protein loss, are on-going.

NCCs originate in the hindbrain and migrate into the craniofacial region to form the maxillary and mandibular jaw structures (Graham, 2002). Several genes were used as markers for different stages of NCC development. *snail1b* and *sox9b* mark NCCs at premigratory stages (Barrallo-Gimeno and Nieto, 2005; Montero-Balaguer *et al.*, 2006). *crestin* marks premigratory and migrating NCCs (Rubinstein *et al.*, 2000) while *dlx2, wnt5a* and *hoxa2* mark migrating NCCs (Akimenko *et al.*, 1994; Ellies *et al.*, 1997; Rauch *et al.*, 1997; Schilling *et al.*, 2001). As shown in Fig. 6, knockdown of *crispld2* altered the pattern of *dlx2* expression compared to uninjected control embryos at 1 dpf. Four distinct clusters of NCCs are seen in uninjected control embryos at 1dpf (Fig 6A). In MO3 injected embryos, *dlx2* expression appears to be upregulated in the NCCs with the most posterior NCC cluster significantly enlarged (Fig. 6B). Ninety percent of MO3 injected embryos showed a larger posterior NCC cluster (by *dlx2* expression) compared to only 34% of control embryos ($p<0.0001$) (Table 2). In addition to the abnormal expression of *dlx2* in NCCs, we observed

abnormal expression of several other NCC cell markers (Figs. 6 and 7 and Table 2). *snail1b* and *wnt5a* expression was significantly increased in MO3 injected embryos (Fig. 6C-F) while *crestin, sox9b*, and *hox2a* expression was decreased (Fig. 7A-F).

Discussion

Previously, we showed that CRISPLD2 is associated with NSCLP in humans and expressed during specific stages of mouse craniofacial development (Chiquet *et al.*, 2007; Letra, 2010). In these studies, zebrafish were used to further define expression and function of Crispld2 during craniofacial development. Amino acid sequence comparison between the zebrafish Crispld2 and CRISPLD2 from other vertebrate species shows a high overall degree of identity (Fig. 1). While there are some sequence differences in the N-terminal region of the protein, this region is relatively divergent between all species. The highest homology identified between species was found to be in the SCP and the LCCL domains (Oyewumi *et al.*, 2003). This high homology between species suggests that Crispld2 could play a similar role in all vertebrates. We found that zebrafish *crispld2* is expressed from 3hpf to 5dpf (Fig. 2). *crispld2* was diffusely expressed in all tissues during early development (5-15 somite stages) and later localized to the craniofacial tissues (1-5 dpf). This expression pattern suggests that *crispld2* might play an important role in overall early development as well as craniofacial development. This is supported by the observation that the complete loss of Crispld2/Lgl1 in mice resulted in embryonic lethality by E9.5 and by our finding that knock down of *crispld2* resulted in lower survival rates at 1dpf and an array of abnormal phenotypes in surviving embryos (Fig. 4).

While heterozygous Crispld2/Lgl1 mice were grossly normal, close examination revealed abnormal lung development with delayed alveolar maturation and disorganization of lung elastin fibers that were trapped in the interstitium (Lan *et al.*, 2009). Oyewumi *et al.* concluded that Crispld2/Lgl1 functions to regulate epithelial-mesenchymal interactions (Oyewumi *et al.*, 2003). Interestingly, epithelial-mesenchymal interactions play an important role in craniofacial development, where neuroepithelial cells programmed to become NCCs must undergo EMT before they can migrate into the craniofacies (Berndt *et al.*, 2008; Kang and Svoboda, 2005). This suggests that Crispld2/Lgl1 might play a role in regulating NCC development and migration. This is supported by our observations that knockdown of *crispld2* resulted in altered NCC clustering at 1dpf (Figs. 6 and 7). NCC clusters, which form the structures of the first and second branchial arches including the Meckel and palatoquadrate cartilages, were abnormal in zebrafish lacking *crispld2* (Figs. 4 and 5). The ceratobranchial cartilages forming the lower jaw are derived from the third through seventh branchial arches (Schilling and Le Pabic, 2009). Interestingly, the ceratobranchial cartilages, which were missing in *crispld2* MO3 injected embryos, are derived from posterior NCC clusters, which were abnormal at 1 dpf (Figs. 6 and 7). Most importantly, we observed varying palatal phenotypes in *crispld2* morpholino injected embryos. Our findings in zebrafish and expression in mice show that CRISPLD2 plays an important role in craniofacial development, and specifically in NCC regulation (Chiquet *et al.*, 2007). While we found that loss of *crispld2* caused perturbation of NCC clusters, as visualized by the abnormal expression of *dlx2, snail1b, wnt5a, crestin, sox9b* and *hoxa2*, it is not known whether this results from abnormal formation, proliferation or migration of NCC cells. Our results show that two different markers for premigratory NCCs are affected differently by *crispld2* knock-down (*snail1b* is increased, while *sox9b* in decreased). We also show that some markers for migrating NCCs are increased (*dlx2* and *wnt5a*) while some are decreased (*hoxa2* and *crestin*) in *crispld2* knock down experiments. This data suggests that *crispld2* plays a role in the specification of some NCC populations. The decrease of *crestin, sox9b* and *hoxa2* expression in *crispld2* morphants suggests that *crispld2* is necessary for the maintenance of a subpopulation of NCCs at the time point examined. However, the increase

of *snail1b, dlx2 and wnt5a* expression at these same time points suggests a complex regulation of NCC specification by *crispld2*. Future studies will determine what specific role *crispld2* plays in epithelial-mesenchymal interactions and NCC specification and migration in the craniofacies.

Craniofacial morphogenesis is a finely tuned process consisting of cell growth, growth factors and receptors, apoptosis and adequate nutrient supply (Nanci, 2003). Perturbation of any of these processes can result in craniofacial dysmorphology. The number of genes that contribute to NSCLP is growing and studies are now focusing on determining the function of these genes in craniofacial development in animal models. In addition, exogenous and endogenous signaling molecules, such as retinoic acid, folic acid and homocysteine, influence craniofacial development, likely through regulating NCCs. Interestingly, these signaling molecules are associated with NSCLP. We have previously shown that genes in the folic acid pathway interact with CRISPLD2 in human NSCLP datasets (Chiquet *et al.*, 2010). This suggests that these pathways may influence CRISPLD2 during craniofacial development and are the focus of our future studies. Our current findings demonstrate a role of *crispld2* in the formation of NCCs and early craniofacial development in zebrafish. Moreover, we suggest that perturbations in genes that regulate NCCs, such as CRISPLD2, can have a detrimental effect on NCC-derived tissues and alter normal craniofacial development, thereby contributing to NSCLP.

Methods

Zebrafish

Zebrafish (Danio rerio) were raised and housed following standard techniques (Westerfield, 1995).

Generation of CRISPLD2 RTPCR and expression probes

Sequence homology of zebrafish CRISPLD2 to other species was assessed using ClustralW2 multiple sequence alignment program (http://www.ebi.ac.uk/Tools/clustalw2/index.html) and BoxShade (http://www.ch.embnet.org/software/BOX_form.html) (Fig. 1, zebrafish accession number: XP_003199065.1) (Larkin *et al.*, 2007). mRNA was isolated from adult zebrafish using phenol-chloroform extraction per standard protocol (Sprague *et al.*, 2006). cDNA was generated using SuperScript™ III Reverse Transcriptase (Invitrogen, Carlsbad, CA). CRISPLD2-specific primers (5'CLD2set1: CGAGGAAAGTGGAAAAGTACAGTA; 3' CLD2set1: GATTGTCTAAAGAACAAACCATCATTA; 5' CLD2set2: CCCAAAATATCAAGTGTGAGAC; 3' CLD2set2: CCATTCTTCAAGGTGCCGG) were used to PCR amplify the DNA probes using the following thermocycler conditions: 30 cycles of 95°C for 30s, (53°C or 57°C, for set 1 and set 2, respectively) for 90s, 68°C for 90s. PCR products were purified (Qiagen, Valencia, CA) and sequenced (LoneStar Labs, Houston, TX). PCR products were then subcloned into Zero Blunt® TOPO® PCR Cloning Kit for Sequencing (Invitrogen, Carlsbad, CA) and then resequenced. Antisense and sense DIG-labeled probes were generated (Roche Cat. No. 11277073910, Switzerland).

Zebrafish were collected at 5-7 and 13-15 somites, 1, 2, 3, 4 and 5 days post fertilization (dpf) for *in situ* hybridization analysis using standard techniques (www.zfin.org) (Sprague *et al.*, 2006). Imaging was performed using LAS Montage Module (Leica, Wetzlar, Germany).

Morpholino (MO)/mRNA injections

Three zebrafish *crispld2* antisense MOs, one mismatch control MO and one p53 MO were designed by GeneTools (Philomath, OR): MO1:TGTAAACAGACTCACTTGTGTGTAG; MO2: TCGATGTCAGGCGGTCTTACTTGGG; MO3:

TTGATGATTTCAGGCCCGGACTCTA; control MO: TTCATCATTTGAGCCCCCGACTCTA; p53 MO: GCGCCATTGCTTTGCAAGAATTG. MO1 targeted the intron/exon junction between exon 3 and intron 3, MO2 targeted the intron/exon junction between exon 4 and intron and MO3 targeted the ATG site in exon 1 (Fig. 3). MOs were diluted in nuclease free water to a stock concentration of 65mg/mL or 2mM. The stock concentration was further diluted with nuclease free water to a working concentration of 12mg/mL. Injections (0.06 - 6 mg/mL) were diluted in Danieu buffer and 0.5 uL of 2% phenol red was added to facilitate injections. One- to two-cell embryos were injected with 1nL of MO and observed during development up to 7 days post fertilization (dpf). A full-length zebrafish *crispld2* cDNA was cloned into the pCS2 vector and *crispld2* mRNA was generated using the mMessage mMachine kit (Ambion). 1 nL of mRNA was injected at a concentration of 100ng/uL. Injection volume was calculated by measuring diameter of injected droplet. Embryos were incubated at 28°C and collected at time points described in text.

In situ hybridization and Alcian Blue staining

Zebrafish embryos were collected at various time points for whole mount *in situ* hybridization expression studies or at 5dpf for cartilage staining using standard techniques (Sprague *et al.*, 2006). Imaging was performed using the LAS Montage Module (Leica, Wetzlar, Germany). Phenotypes were categorized based on jaw and palatal structures into mild (abnormal structure) and severe (loss of structure(s)) categories. In the NCCs, *dlx2* expression was assessed based on size of expression domain compared to the UICs. Chi square statistic was used to test for differences in all analyzes.

Western Blot

Cell lysates were prepared from UIC and MO3 injected embryos reaching approximately high stage (3.33 hpf) and dechorionated with pronase. After de-yolking manually on an agarose plate, the embryos were collected and mixed with SDS sample buffer and boiled for 10 minutes. Proteins were resolved by electrophoresis then transferred from a SDS-PAGE gel onto a polyvinylidene difluoride (PVDF) membrane. The membrane was incubated with primary antibodies: anti-Crispld2 (1:200 dilution) and anti-Gapdh (1:250 dilution) at room temperature for 2h. Following washing three times with 1xTBST for 15 minutes each, the membrane was incubated with secondary anti-rabbit conjugated to horseradish peroxidase (HRP) (1:20,000 dilution) for 1 hour at room temperature. Proteins bands were visualized using SuperSignal West Pico Chemiluminescent Substrate according to the manufacturer's protocol. Anti-Crispld2 was generated in rabbit using peptide SLELRQLMQRYQEELE from the N-terminus of zebrafish Crispld2 as the immunogen (Thermo Scientific, Rockford, IL). Rabbit polyclonal antibody to Gapdh (gluceraldehide-3-phosphate dehydrogenase) was purchased from GeneTex (Cat # GTX124502, Irvine, CA). Secondary antibody HRP-goat anti-rabbit IgG was purchased from Invitrogen (Cat# 656120, Grand Island, NY). SuperSignal West Pico Chemiluminescent Substrate was purchased from Thermo Scientific (Rockford, IL).

Supplementary Material

Refer to Web version on PubMed Central for supplementary material.

Acknowledgments

We thank Drs. Dan Wagner and Mary Ellen Lane for the use of their zebrafish facilities at Rice University (Houston, Texas). This work is supported by NIH grants R01-DE011931 to JTH and F30-DE019343 to BTC.

References

Akimenko MA, Ekker M, Wegner J, Lin W, Westerfield M. Combinatorial expression of three zebrafish genes related to distal-less: part of a homeobox gene code for the head. J Neurosci. 1994; 14:3475–3486. [PubMed: 7911517]

Barrallo-Gimeno A, Nieto MA. The Snail genes as inducers of cell movement and survival: implications in development and cancer. Development. 2005; 132:3151–3161. [PubMed: 15983400]

Berndt JD, Clay MR, Langenberg T, Halloran MC. Rho-kinase and myosin II affect dynamic neural crest cell behaviors during epithelial to mesenchymal transition in vivo. Dev Biol. 2008; 324:236–244. [PubMed: 18926812]

Blanton SH, Cortez A, Stal S, Mulliken JB, Finnell RH, Hecht JT. Variation in IRF6 contributes to nonsyndromic cleft lip and palate. Am J Med Genet A. 2005; 137:259–262. [PubMed: 16096995]

Chiquet BT, Henry R, Burt A, Mulliken JB, Stal S, Blanton SH, Hecht JT. Nonsyndromic cleft lip and palate: CRISPLD genes and the folate gene pathway connection. Birth Defects Res A Clin Mol Teratol. 2010 in press.

Chiquet BT, Lidral AC, Stal S, Mulliken JB, Moreno LM, Arco-Burgos M, Valencia-Ramirez C, Blanton SH, Hecht JT. CRISPLD2: A Novel NSCLP Candidate Gene. Hum Mol Genet. 2007; 16:2241–2248. [PubMed: 17616516]

Ellies DL, Langille RM, Martin CC, Akimenko MA, Ekker M. Specific craniofacial cartilage dysmorphogenesis coincides with a loss of dlx gene expression in retinoic acid-treated zebrafish embryos. Mech Dev. 1997; 61:23–36. [PubMed: 9076675]

Gorlin, RJ.; Cohen, MM.; Hennekam, RCM. Syndromes of the Head and Neck. Fourth Edition. New York: Oxford University Press; 2001.

Graham A. Jaw development: chinless wonders. Curr Biol. 2002; 12:R810–812. [PubMed: 12477407]

Jugessur A, Rahimov F, Lie RT, Wilcox AJ, Gjessing HK, Nilsen RM, Nguyen TT, Murray JC. Genetic variants in IRF6 and the risk of facial clefts: single-marker and haplotype-based analyses in a population-based case-control study of facial clefts in Norway. Genet Epidemiol. 2008; 32:413–424. [PubMed: 18278815]

Kang P, Svoboda KK. Epithelial-mesenchymal transformation during craniofacial development. Journal of dental research. 2005; 84:678–690. [PubMed: 16040723]

Kaplan F, Ledoux P, Kassamali FQ, Gagnon S, Post M, Koehler D, Deimling J, Sweezey NB. A novel developmentally regulated gene in lung mesenchyme: homology to a tumor-derived trypsin inhibitor. Am J Physiol. 1999; 276:L1027–1036. [PubMed: 10362728]

Lan J, Ribeiro L, Mandeville I, Nadeau K, Bao T, Cornejo S, Sweezey NB, Kaplan F. Inflammatory cytokines, goblet cell hyperplasia and altered lung mechanics in Lgl1+/- mice. Respir Res. 2009; 10:83. [PubMed: 19772569]

Larkin MA, Blackshields G, Brown NP, Chenna R, McGettigan PA, McWilliam H, Valentin F, Wallace IM, Wilm A, Lopez R, Thompson JD, Gibson TJ, Higgins DG. Clustal W and Clustal X version 2.0. Bioinformatics. 2007; 23:2947–2948. [PubMed: 17846036]

Letra A, Menezes R, Cooper M, Fonseca R, Tropp S, Govil M, Granjeiro J, Imoehl S, Mansilla M, Murray J, Castilla E, Orioli I, Czeizel AE, Ma L, Chiquet B, Hecht J, Vieira A, Marazita M. Crispld2 Variants Including a C471t Silent Mutation May Contribute to Nonsyndromic Cleft Lip with or without Cleft Palate. Cleft Palate Craniofac J. 2010

Letra A, Menezes R, Cooper ME, Fonseca RF, Tropp S, Govil M, Granjeiro JM, Imoehl SR, Mansill MA, Murray JC, Castilla EE, Orioli IM, Czeizel AE, Ma L, Chiquet BT, Hecht JT, Vieira AR, Marazita ML. *CRISPLD2* variants including a C471T silent mutation may contribute to nonsyndromic cleft lip with or without cleft palate. Cleft Palate Craniofacial Journal. 2010 In Press.

Montero-Balaguer M, Lang MR, Sachdev SW, Knappmeyer C, Stewart RA, De La Guardia A, Hatzopoulos AK, Knapik EW. The mother superior mutation ablates foxd3 activity in neural crest progenitor cells and depletes neural crest derivatives in zebrafish. Dev Dyn. 2006; 235:3199–3212. [PubMed: 17013879]

Nanci, A. Ten Cate's Oral Histology - Development, Structure, and Function. 6. Los Angelos: Mosby; 2003.

Oyewumi L, Kaplan F, Sweezey NB. Lgl1, a mesenchymal modulator of early lung branching morphogenesis, is a secreted glycoprotein imported by late gestation lung epithelial cells. The Biochemical journal. 2003; 376:61–69. [PubMed: 12880386]

Park JW, McIntosh I, Hetmanski JB, Jabs EW, Vander Kolk CA, Wu-Chou YH, Chen PK, Chong SS, Yeow V, Jee SH, Park BY, Fallin MD, Ingersoll R, Scott AF, Beaty TH. Association between IRF6 and nonsyndromic cleft lip with or without cleft palate in four populations. Genetics in Medicine. 2007; 9:219–227. [PubMed: 17438386]

Rauch GJ, Hammerschmidt M, Blader P, Schauerte HE, Strahle U, Ingham PW, McMahon AP, Haffter P. Wnt5 is required for tail formation in the zebrafish embryo. Cold Spring Harb Symp Quant Biol. 1997; 62:227–234. [PubMed: 9598355]

Robu ME, Larson JD, Nasevicius A, Beiraghi S, Brenner C, Farber SA, Ekker SC. p53 activation by knockdown technologies. PLoS Genet. 2007; 3:e78. [PubMed: 17530925]

Rubinstein AL, Lee D, Luo R, Henion PD, Halpern ME. Genes dependent on zebrafish cyclops function identified by AFLP differential gene expression screen. Genesis. 2000; 26:86–97. [PubMed: 10660676]

Scapoli L, Palmieri A, Martinelli M, Pezzetti F, Carinci P, Tognon M, Carinci F. Strong evidence of linkage disequilibrium between polymorphisms at the IRF6 locus and nonsyndromic cleft lip with or without cleft palate, in an Italian population. Am J Hum Genet. 2005; 76:180–183. [PubMed: 15558496]

Schilling TF, Le Pabic P. Fishing for the signals that pattern the face. J Biol. 2009; 8:101. [PubMed: 20067597]

Schilling TF, Prince V, Ingham PW. Plasticity in zebrafish hox expression in the hindbrain and cranial neural crest. Dev Biol. 2001; 231:201–216. [PubMed: 11180963]

Shen X, Liu RM, Yang L, Wu H, Li PQ, Liang YL, Xie XD, Yao T, Zhang TT, Yu M. The CRISPLD2 gene is involved in cleft lip and/or cleft palate in a Chinese population. Birth defects research. Part A, Clinical and molecular teratology. 2011; 91:918–924.

Sprague J, Bayraktaroglu L, Clements D, Conlin T, Fashena D, Frazer K, Haendel M, Howe DG, Mani P, Ramachandran S, Schaper K, Segerdell E, Song P, Sprunger B, Taylor S, Van Slyke CE, Westerfield M. The Zebrafish Information Network: the zebrafish model organism database. Nucleic acids research. 2006; 34:D581–585. [PubMed: 16381936]

Srichomthong C, Siriwan P, Shotelersuk V. Significant association between IRF6 820G->A and non-syndromic cleft lip with or without cleft palate in the Thai population. J Med Genet. 2005; 42:e46. [PubMed: 15994871]

Vieira AR, Cooper ME, Marazita ML, Orioli IM, Castilla EE. Interferon regulatory factor 6 (IRF6) is associated with oral-facial cleft in individuals that originate in South America. Am J Med Genet A. 2007; 143A:2075–2078. [PubMed: 17702008]

Westerfield, M. The zebrafish book : a guide for the laboratory use of zebrafish (Danio rerio). 3. Eugene, OR: M Westerfield; 1995.

Wyszynski, D., editor. Cleft Lip and Palate: From Origin to Treatment. Oxford: Oxford University Press; 2002.

Zucchero TM, Cooper ME, Maher BS, Daack-Hirsch S, Nepomuceno B, Ribeiro L, Caprau D, Christensen K, Suzuki Y, Machida J, Natsume N, Yoshiura K, Vieira AR, Orioli IM, Castilla EE, Moreno L, Arcos-Burgos M, Lidral AC, Field LL, Liu YE, Ray A, Goldstein TH, Schultz RE, Shi M, Johnson MK, Kondo S, Schutte BC, Marazita ML, Murray JC. Interferon regulatory factor 6 (IRF6) gene variants and the risk of isolated cleft lip or palate. N Engl J Med. 2004; 351:769–780. [PubMed: 15317890]

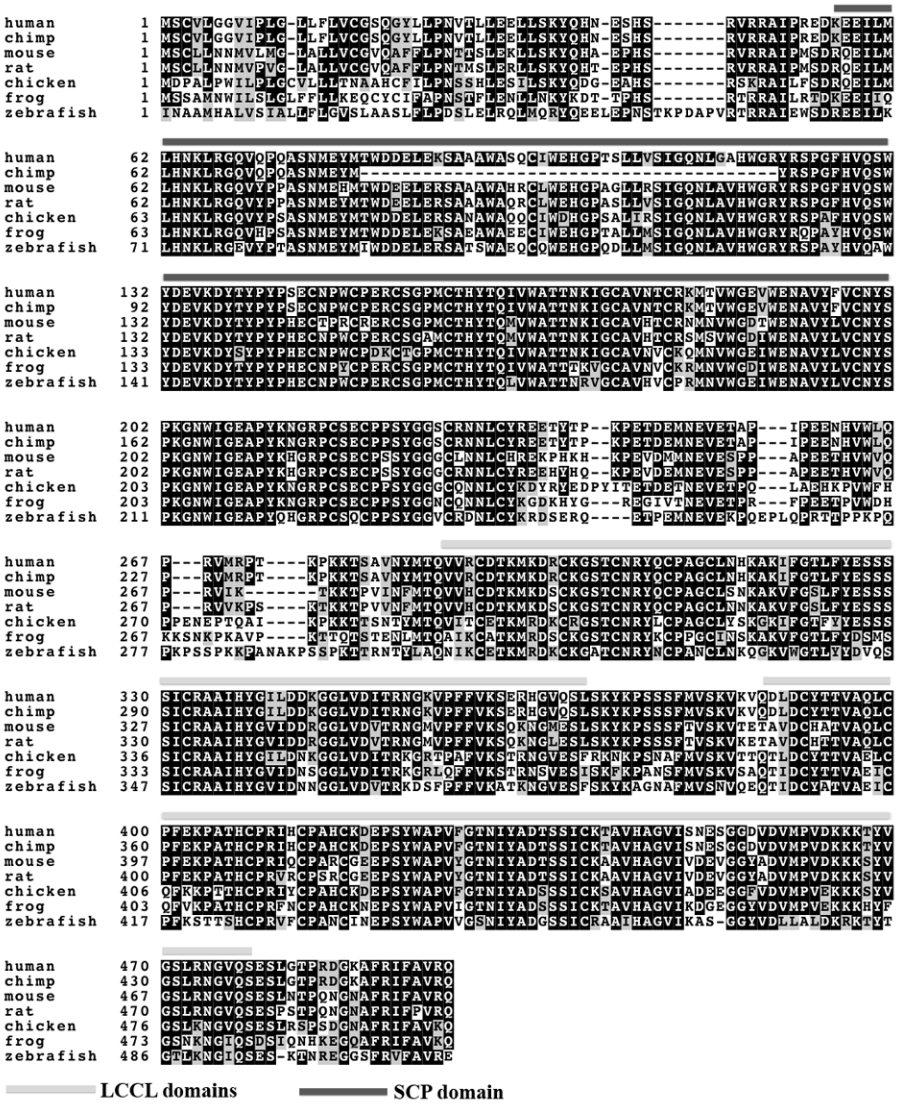

Fig. 1. CRISPLD2 amino acid alignment across vertebrate species

Black boxes indicate >50% of sequences have the identical amino acid; Grey boxes indicate >50% of sequences have a conserved substitution. Shaded lines mark above the sequence marks the LCCL domains and the SCP domain. It is unclear whether isoleucine is utilized as an alternative initiation codon at position 1 or if the methionine at position 5 is the actual initiation codon. Accession numbers: human - NP_113664, chimp - XP_001152165.2, mouse - NP_084485, rat - NP_612527, chicken - XP_414180, frog (X. tropicalis) - NP_001027499, zebrafish - XP_003199065.

Fig. 2. *crispld2* expression during zebrafish development

(A) Detection of *crispld2* mRNA by RTPCR during early development (NTC = no template control, UWT = unfertilized wild type embryo, dpf = days post fertilization, hpf = hrs post fertilization). (B-H) *in situ* hybridization showing *crispld2* expression (purple) at the following stages: (B) 5-7 somite, (C) 13-15 somite, (D) 1 dpf, (E) 2 dpf, (F) 3 dpf, (G) 4 dpf, and (H) 5 dpf.

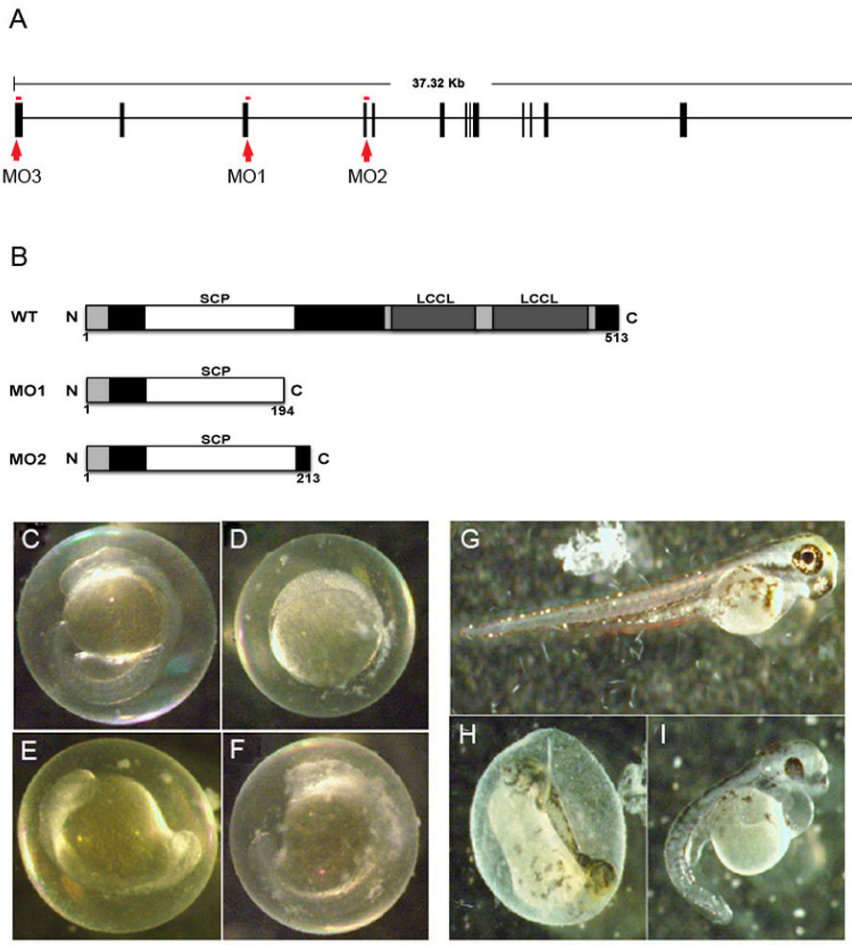

Fig. 3. Morpholino knockdown of *crispld2*

(A) Genomic architecture of c*rispld2* showing MO1(1), MO2(2) and MO3(3) targets (boxes = exons). MO1 and MO2 are splice site morpholinos. MO3 is a start site morpholino. (B) Diagram showing predicted truncated proteins generated by splice site morpholinos, MO1 and MO2, compared to wild type. (C-I) Examples of phenotypes of c*rispld2* MO injected embryos are shown. (C) Uninjected control (UIC) embryo at 1 dpf. (D-F) various MO phenotypes at 1 dpf. (G) UIC embryo at 5 dpf. (H, I) MO phenotypes at 5 dpf.

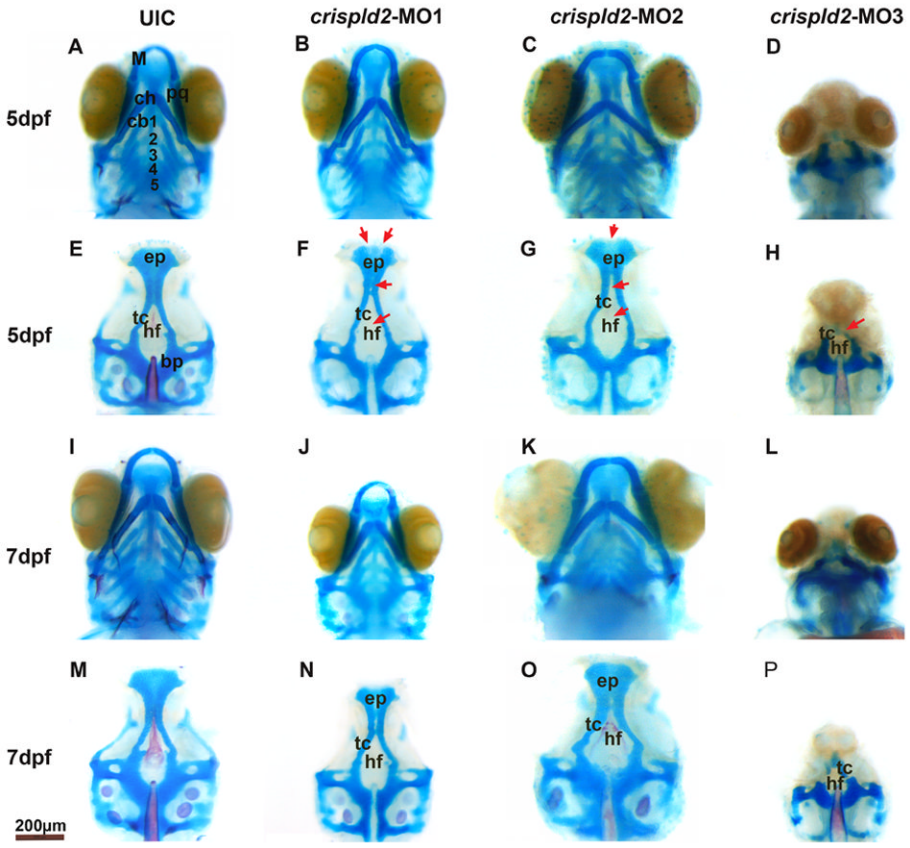

Fig. 4. Knock down of *crispld2* causes craniofacial abnormalities

Alcian blue and alizarin red staining at 5 dpf and 7 dpf shows structural palatal and jaw abnormalities in *crispld2* MO knockdown zebrafish. For all images, upper picture (A-D and I-L) shows embryo with jaw and lower picture shows the palate after jaw removal (E-H and M-P). A, E, I and M are uninjected control (UIC) embryos. B-D, F-H, J-L and N-P show the phenotypes associated with knock down of *crispld2*. The range of palatal abnormalities is shown (red arrowheads) in F-H and N-P. Specifically, in MO1 injected embryos (F and N), there is a loss of the hypophyseal fenestra as well as malformations of the trabeculae and the ethmoid plate. In MO2 injected embryos (G and O), there are malformations of the hypophyseal fenestra, the trabeculae and the ethmoid plate. In MO3 injected embryos (H and P), there is a loss of the hypophyseal fenestra, severe malformations of the trabeculae and a loss of the ethmoid plate. bp, basal plate; cb, ceratobranchial; ch, ceratohyal; ep, ethmoid plate; hf, hypophyseal; fenestra M, Meckel; pq, palatoquadrate; tc, trabeculae. Scale bar = 200 nm.

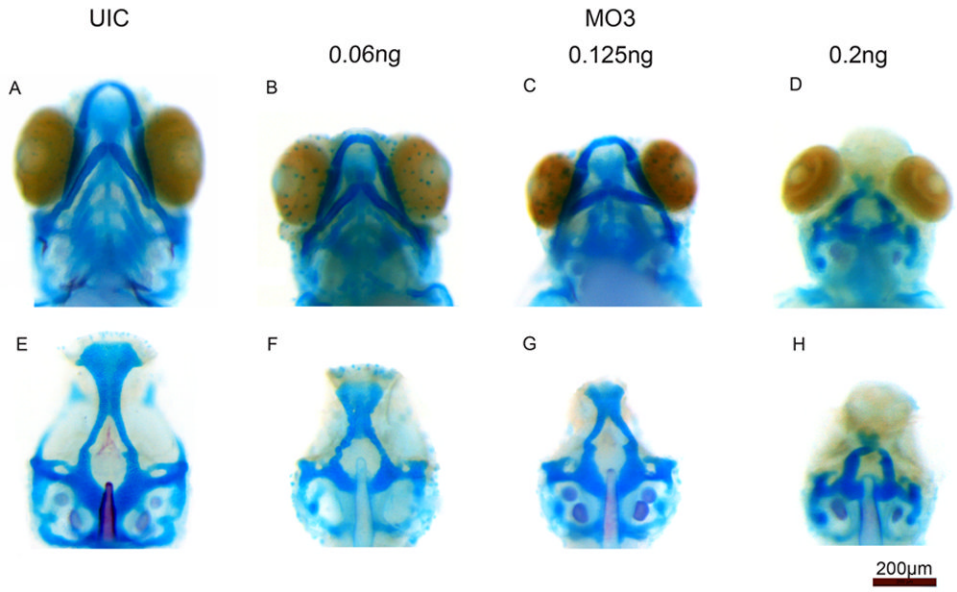

Fig. 5. Cartilage abnormalities are increased with increasing amount of MO3 injected

Alcian blue staining at 5 dpf shows increasingly abnormal cartilage elements as the amount of MO3 is increased. For all images, upper picture shows embryo with jaw and lower picture shows the palate after jaw removal. A and E are uninjected control (UIC) embryos. B-D and F-H show increasing amounts of MO3 injected. The highest amount of MO3 (0.2ng) results in a complete loss of the lower jaw and substantial malformation of the palate.

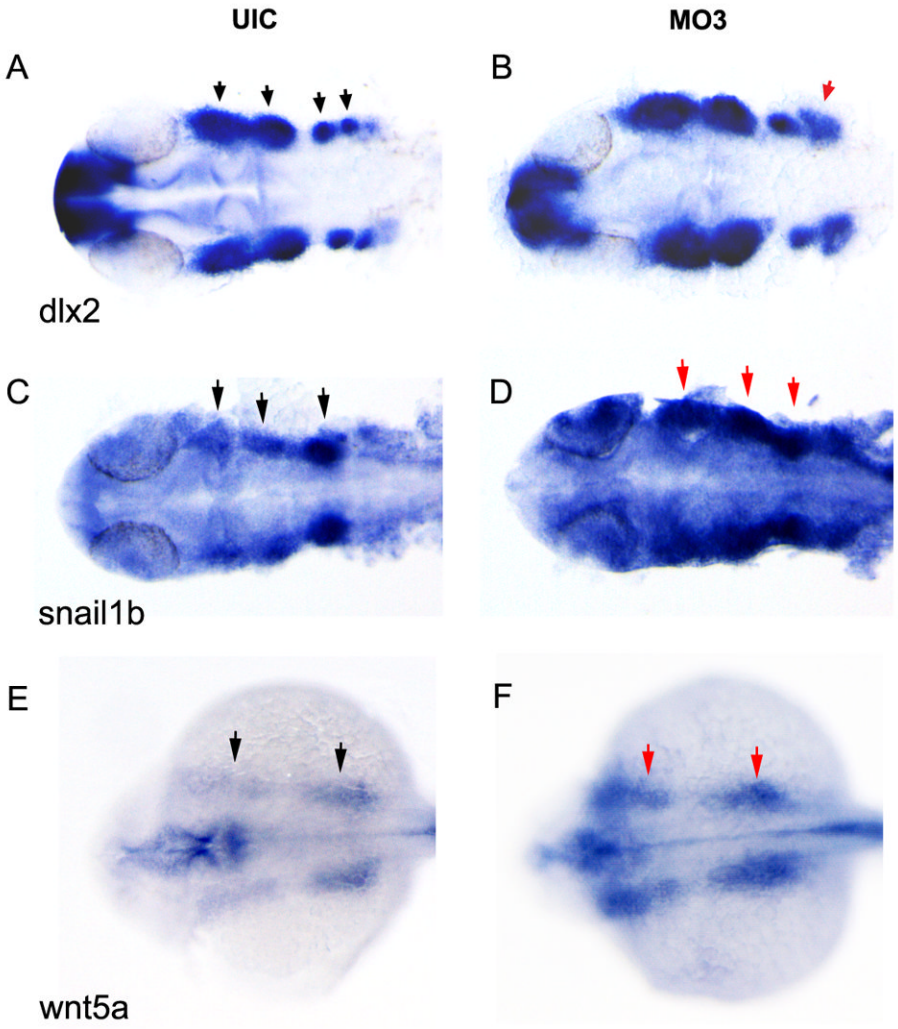

Fig. 6. Increased NCC marker expression in *crispld2* knockdown embryos

dlx2, snail1b and wnt5a expression is visualized by whole mount *in situ* staining at approximately 1 dpf. (A, C and E) *dlx2, snail1b and wnt5a* expression in UIC and (B, D and F) *dlx2, snail1b and wnt5a* expression in *crispld2* MO3 embryos. MO3 injected at 2ng/embryo. Black arrows on uninjected control (UIC) show NCC clusters; red arrows denote areas of increased expression.

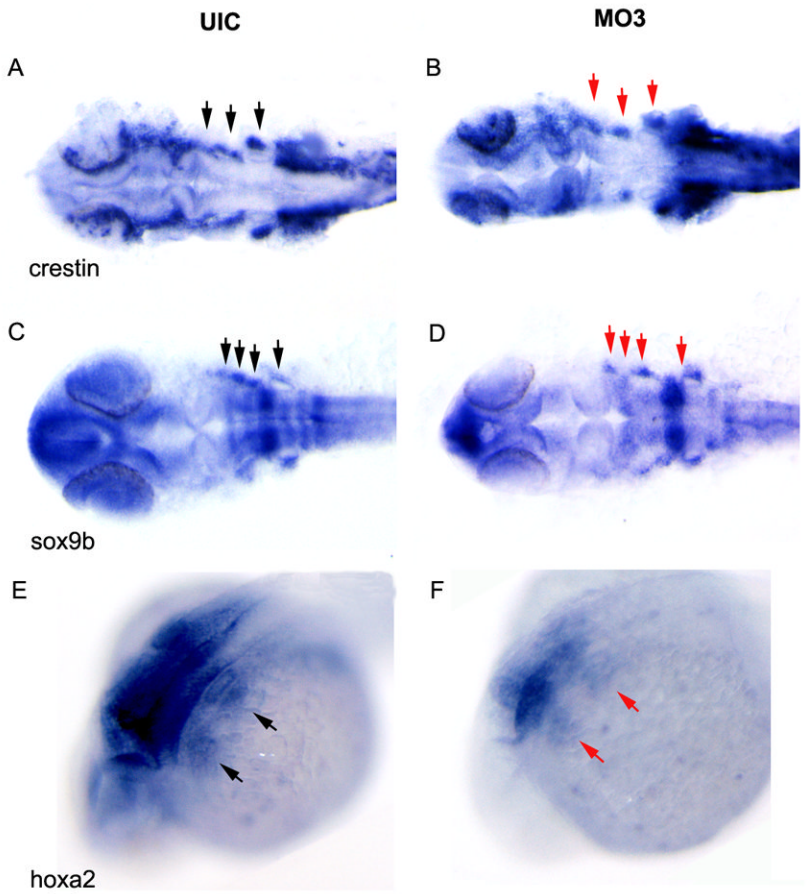

Fig. 7. Decreased NCC marker expression in *crispld2* knockdown embryos

crestin, sox9b and *hoxa2* expression was visualized by whole mount *in situ* staining at approximately 1 dpf. (A, C and E) *crestin, sox9b* and *hoxa2* expression in UIC and (B, D, and F) *crestin, sox9b* and *hoxa2* expression in *crispld2* MO3 embryos. MO3 injected at 2ng/embryo. Black arrows on uninjected control (UIC) show NCC clusters; red arrows denote areas of decreased expression.

Table 1

Classification of zebrafish phenotype

	Normal	Mild	Severe	Total	*P* value
UIC	48 (96%)	2 (4%)	0 (0%)	50 (100%)	-
MO1 (6ng)	22 (44%)	27 (54%)	1 (2%)	50	<0.0001
MO2 (0.5ng)	16 (32%)	15 (30%)	19 (38%)	50	<0.0001
MO3 (0.2ng)	6 (12%)	8 (16%)	36 (72%)	77	<0.0001
	1(4%)	1(4%)	25(92%)		
MO3MM (1ng)	49 (98%)	1 (2%)	0 (0%)	50	0.8437

Table 2

Expression of NCC markers

		Normal	Abnormal	*p* value
dlx2	MO3	10 (10%)	95 (90%)	<0.0001
	UIC	61 (66%)	31 (34%)	
snail1b	MO3	22 (32%)	47 (68%)	<0.0001
	UIC	50 (86%)	8 (14%)	
wnt5a	MO3	13 (34%)	25 (66%)	<0.0001
	UIC	21 (88%)	3 (12%)	
crestin	MO3	14 (21%)	53 (79%)	<0.0001
	UIC	40 (67%)	20 (33%)	
sox9b	MO3	14 (19%)	61 (81%)	<0.0001
	UIC	50 (79%)	13 (21%)	
hoxa2	MO3	10 (13%)	65 (87%)	<0.0001
	UIC	55 (71%)	22 (29%)	